Bouayad, F.E., El Idrysy, M., Ouallali, A., El Amrani, M., Courba, S., Hahou, Y., Benhachmi, M.K., Spalevic, V., Kebede F. Briak, H. (2023). Assessing soil erosion dynamics in the Rmel watershed, northern Morocco by using the RUSLE model, GIS, and remote sensing integration. Agriculture and Forestry, 69 (4): 173-194. doi:10.17707/AgricultForest.69.4.11

DOI: 10.17707/AgricultForest.69.4.11

Fatima Ezzahraa BOUAYAD, Majda EL IDRYSY, Abdessalam OUALLALI, Mohamed EL AMRANI, Said COURBA, Youssef HAHOU, Mohammed Karim BENHACHMI, Velibor SPALEVIC, Fassil KEBEDE, Hamza BRIAK [1]

ASSESSING SOIL EROSION DYNAMICS IN THE RMEL WATERSHED, NORTH-WESTERN MOROCCO BY USING THE RUSLE MODEL, GIS, AND REMOTE SENSING INTEGRATION

SUMMARY

Soil erosion induced by water constitutes a challenge with far-reaching environmental and socioeconomic implications across diverse global regions. This phenomenon detrimentally affects agricultural yield, accelerates dam siltation, and amplifies the susceptibility to flooding. Consequently, a prerequisite for any land development initiative is the meticulous identification and mapping of areas prone to erosion. The Revised Universal Soil Loss Equation (RUSLE) is the predominant method for evaluating soil erosion, encompassing climate erosivity, topography, vegetation cover, soil erodibility, and anti-erosion interventions. This study integrated RUSLE with Geographic Information Systems (GIS) to delineate soil losses within the Rmel watershed in north-western Morocco. The outcomes unveiled an average annual erosion rate of approximately 15.8 tons per hectare, a comparatively modest figure with adjacent regions. Merely 9% of the watershed exhibits vulnerability to soil erosion, surpassing the threshold of 15 tons per hectare annually. These vulnerable areas are predominantly influenced by anthropogenic activities in the basin's central region and adverse climatic conditions downstream. The insights from this research can inform decision-makers in developing strategic action plans and policies for effective soil erosion management in the region. Additionally, the integration of magnetic susceptibility could serve as a complementary tool to enhance the robustness of this analysis.

Keywords: Soil erosion, RUSLE model, GIS, Rmel watershed, Morocco.

[1] Fatima Ezzahraa Bouayad (corresponding author: fatimabouay@gmail.com), Abdessalam Ouallali, Mohammed Karim Benhachmi, Process Engineering and Environment Laboratory, Faculty of Sciences and Techniques of Mohammedia, Hassan II University of Casablanca, BP 146, Mohammedia 28806, MOROCCO; Majda El Idrysy, Mohamed El Amrani, Said Courba, Youssef Hahou, Laboratory of Geosciences, Water and Environment, Department of Geology, Faculty of Sciences, Mohammed V University in Rabat, 4 Avenue Ibn Batouta, BP. 1014 R.P., 10000, Rabat, MOROCCO; Velibor Spalevic, Biotechnical Faculty, University of Montenegro, Podgorica, MONTENEGRO; Fassil Kebede, Hamza Briak, Center of Excellence for Soil and Fertilizer Research in Africa (CESFRA), Mohammed VI Polytechnic University, 660 Lot, Ben Guerir 43150, MOROCCO.

Note: The authors declare that they have no conflicts of interest. Authorship Form signed online.
Received: 05/10/2023 *Accepted: 27/11/2023*

INTRODUCTION

Water erosion, resulting from the degradation of surface soil layers and the displacement of constituent materials (Rodrigues Neto, 2022; Spalevic, 2011, Kavian *et al.* 2018), occurs due to energy release induced by raindrop impact, wind, glaciers, and soil particle transportation (Bhat *et al.* 2019). This widespread phenomenon inflicts significant environmental damage, profoundly affecting ecological and socioeconomic aspects (Moukhchane *et al.* 1998; Spalevic *et al.*, 2013; Saikumar *et al.* 2022; Sabri *et al.* 2022). Globally, erosion poses a serious threat, particularly in Mediterranean countries where factors such as irregular rainfall, elevated temperatures, and a topography characterized by hills and mountains exacerbate soil vulnerability (García-Ruiz *et al.* 2013; Ouallali *et al.* 2020; Salhi *et al.* 2023). A 1977 FAO study revealed that 12.6 million hectares of crops and rangelands in Morocco were at risk of water erosion (El Jazouli *et al.* 2019; Fartas *et al.* 2022). A subsequent 1990 FAO study indicated a worsening scenario, with water erosion affecting 40% of the land area.

Water erosion is the foremost menace to soil degradation in Morocco, with annual soil loss generally exceeding 50 t/ha/y (Salhi *et al.* 2021). The Moroccan mountains present complex erosion challenges, including sheet erosion, gullying, soil movement, bank undermining, solifluction, and mudflows (Roose, 2002). The Rif region experiences a more insidious form of erosion, impacting soil fertility and dam reservoir water volume due to silting (Ouallali *et al.* 2020).

Despite the topographical, lithological, and climatic characteristics of the Oued Rmel watershed, it is not impervious to water erosion phenomena. Integrating remote sensing and Geographic Information Systems (GIS) emerges as crucial tools in interactive decision support and operational planning for risk management operations.

Soil erosion modelling is one of the steps used to plan suitable soil protection measures and detect erosion hotspots (Bezak et *al.* 2021). Various methods exist to determine erosion rates or states, including hydrological modelling methods (Briak *et al.* 2016), geochemical tracers (Guzmán *et al.* 2013), surface geophysical techniques (Ibrahim *et al.* 2020), magnetic susceptibility (Ouallali *et al.* 2023), and empirical modelling (Spalevic *et al.* 2013; Sakuno *et al.* 2020), with the Universal Soil Loss Equation (USLE), its modified version (MUSLE), and its revised version (RUSLE) being the most widely employed (Zhang *et al.* 2009; Gwapedza *et al.* 2018; Djoukbala *et al.* 2019). The optimal model selection depends on the study area's variability and data availability (Stefanidis *et al.* 2022).

The USLE/RUSLE model, grounded in mathematical equations applied in field observations and laboratory analyses, stands among the foremost mathematical models for predicting soil erosion losses (Römkens *et al.* 2015; Ed-daoudy *et al.* 2023). The RUSLE model computes the long-term average annual erosion rate by factoring in rainfall, soil type, topography, vegetation cover, and erosion control practices, allowing for a thorough assessment of erosional impact over time.

This study's primary objective is to determine and map sediment-producing areas in the Rmel watershed. The study also looked into the repercussions of erosion on the water potential of the Rmel dam. The dam, pivotal in providing irrigation and potable water, is also crucial in flood protection for the Tangier-Med port and Ksar Essghir. Through this investigation, we aim to show the complex interaction between erosion dynamics and the essential functions of the Rmel dam in sustaining agricultural, residential, and industrial needs in the region.

MATERIAL AND METHODS

Study area

The Oued Rmel watershed is situated in northwest Morocco, within the province of Ksar Essghir in the Rif region, approximately 44 km northeast of Tangier (Figure 1).

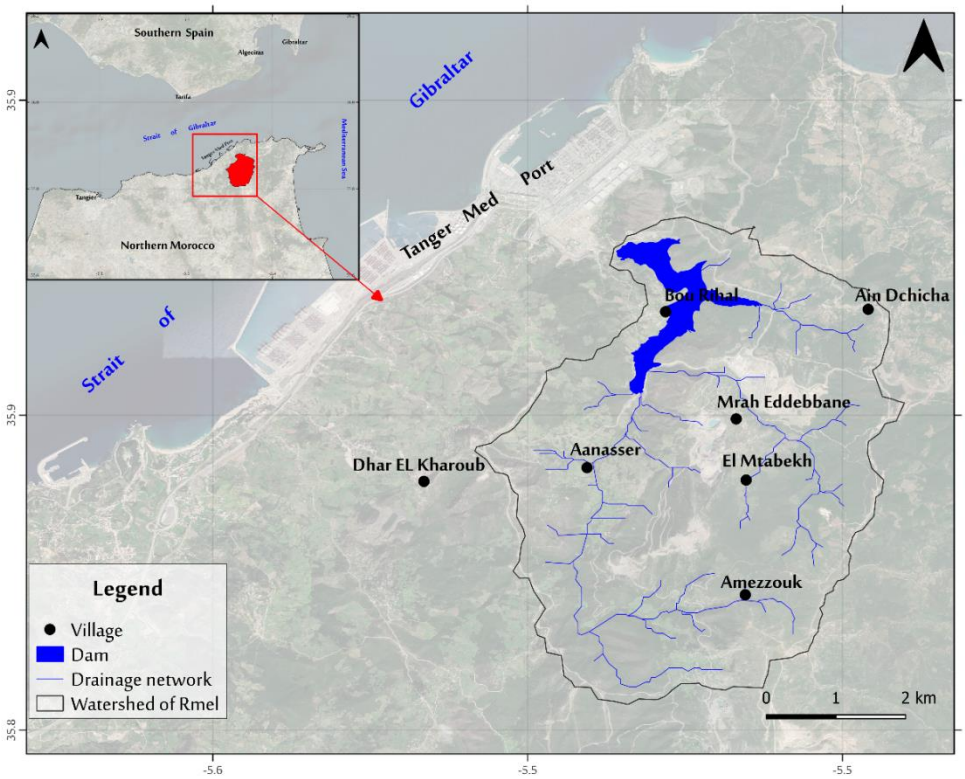

Fig 1: Localization map of the study area

A prominent hydraulic structure in this area is the Rmel dam, constructed in 2008 along the main river. This dam is paramount for hydroelectric power generation, irrigation, water supply, and flood prevention. Boasting a storage capacity of up to 400 million cubic meters, it plays a pivotal role in regional water resource management.

The hydrographic network of the Rmel basin spans a total length of 12.7km and is nourished by rainwater and mountain streams. The primary river within the basin is the Oued Rmel. The climate in the Rmel watershed is categorized as subhumid. Climatic data reveals an average annual rainfall of approximately 400mm, with notable variability from one year to the next, occasionally leading to severe drought conditions. The heaviest rainfall typically occurs in January and February. The region experiences an average temperature of around 17.8°C, with peak temperatures reaching 29.3°C in summer and minimum temperatures averaging 6.3°C in winter. Geologically, the Rmel watershed is characterized by sedimentary deposits, primarily composed of limestone, sandstone, marl, and clay, spanning from the Paleozoic to the Quaternary age. This geological composition contributes to the diverse landscape and environmental dynamics observed in the region.

Model implementation

Various models, differing in complexity and data prerequisites, offer the capability to estimate soil erosion (Karydas *et al.* 2014). These models are versatile in forecasting soil erosion rates across diverse temporal and spatial scales. Notably, the Universal Soil Loss Equation (USLE) model underwent refinement, evolving into the Revised Universal Soil Loss Equation (RUSLE) (Millward & Mersey, 1999).

This updated model facilitates the assessment of the average annual rate of soil loss and allows for the determination of the spatial distribution of an erosion risk map (Mukanov *et al.* 2019). Widely recognized as the preeminent model for estimating soil loss, the RUSLE guides efforts toward soil conservation to mitigate water erosion. The successful application of this novel model hinges on incorporating diverse data types that accurately capture field conditions. We employed the RUSLE model to pursue our research goals, following the outlined protocol depicted in Figure 2.

According to the RUSLE model (Eq. (1)), soil loss (A) is a multiplicative function based on five elements: topography factor (LS), vegetation cover factor (C), soil erodibility (K) (t.h/MJ.mm), rainfall erosivity (R) (MJ.mm/ha.h.year), and erosion control practices factor (P) interrelated according to the equation:

$$A=R*K*LS*C*P \quad \text{Eq. (1)}$$

with:

A: is the average soil erosion per surface unit (t/h/year);
R: is the rainfall and runoff erosivity factor (Mjmm/ha-H-year);
LS: is the slope length (L) and slope steepness (S)factor;
K: is the soil erodibility factor (t-ha-h/ha-MJ-mm);
C: is vegetation cover, management, and culture practices factor;
P: is the conservation practice factor.

We used different data from several sources to evaluate water erosion in the study area. We describe these data in Table 1.

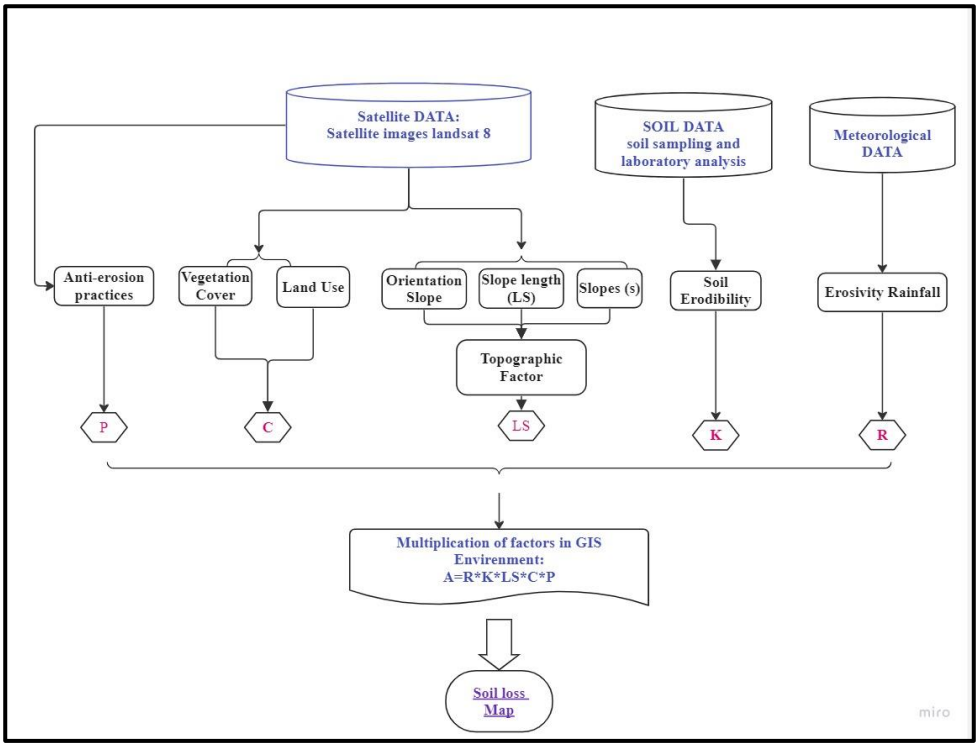

Fig 2: The RUSLE methodology flowchart.

Table 1: Description of datasets used for the RUSLE model.

Datasets	Data source
Rainfall data for the 2010-2022 period recorded at the Tanger Med, Ksar Essghir, Oued Rmel, Alian, Elhorra	ABHL
Data on vegetation cover extracted from Landsat 8 Oli satellite image (no. 201035), downloaded on 05/31/2022	Earth explorer
Topographic data from ASTER 30m digital terrain model (DEM)	Earthdata
Field observations and laboratory analysis of soil samples.	Sample analysis at the laboratory Field observations

To acquire the foundational data essential for constructing maps of water erosion variables in the Oued Rmel watershed, a series of analysis and processing activities are imperative for each component. To estimate soil erosion, a comprehensive dataset of rainfall spanning 12 years (2010-2022) was procured from five stations—Tangier Med, Ksar Essghir, Oued Rmel, Alian, and Elhorra—courtesy of the Loukkos Water Basin Agency. This dataset was instrumental in calculating the rainfall-runoff erosion factor (R factor).

In crafting a rainfall erosion map for the watershed, the rainfall erosion point data underwent interpolation using the Inverse Distance Weighted (IDW) method. This deterministic interpolation method, reliant on the influence of distance for climate station sites, was scrutinized and deemed effective for computing the erosion factor. The resulting R-factor elucidates the spatial distribution of rainfall aggression across the entire area.

Soil type data were employed to assess the soil erodibility factor K. A total of 48 soil samples were meticulously collected in the field and subsequently subjected to physical (particle size analysis) and chemical (organic matter, pH, and electrical conductivity) analyses. These analytical procedures were conducted at the soil chemistry and physics laboratory of the "*Environnement et Conservation des Ressources Naturelles*" research unit at the Rabat Regional Agricultural Research Centre (INRA), contributing to the production of the soil erodibility information layer. The Rmel basin encompasses four primary soil types: vertisol, fluviosol, lithosol, and calcimagnesic soil, as illustrated in Figure3. Each soil type contributes to the basin's diverse and complex soil composition, influencing the local ecosystem and land use characteristics.

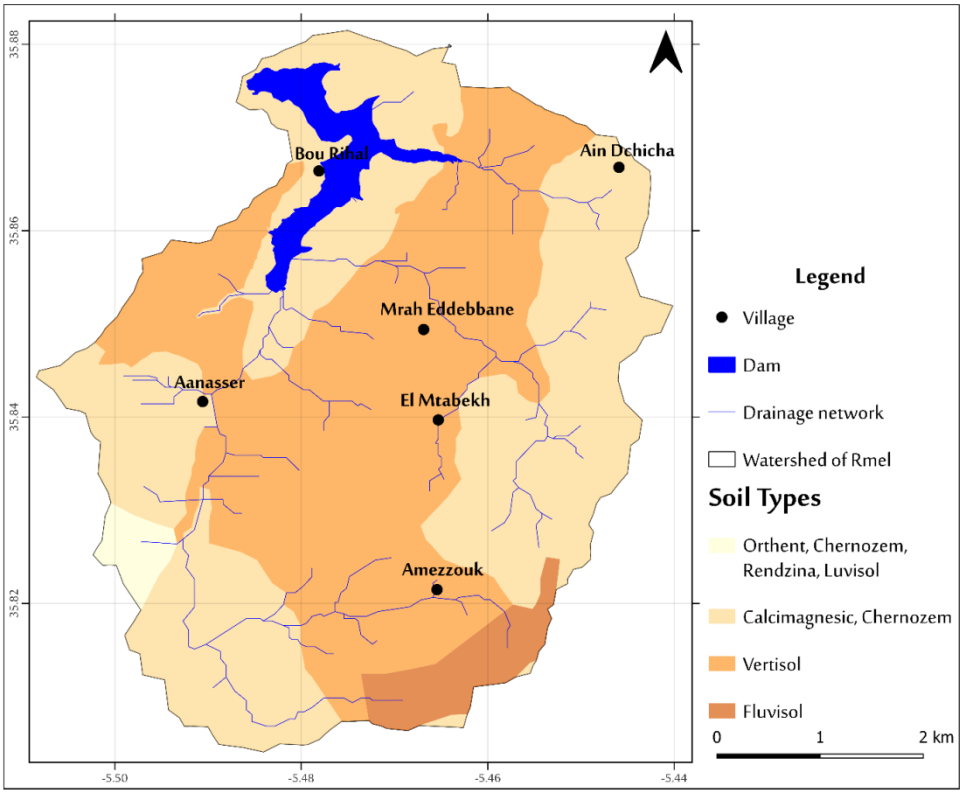

Fig 3: Soil map of the Rmel basin.

On 05/31/2022, a Landsat 8 satellite image was acquired and subsequently subjected to supervised classification using ENVI image processing software.

This process yielded a map illustrating land use unit distribution and the Normalized Difference Vegetation Index (NDVI) calculation. The Rmel watershed exhibits diverse land uses, showcasing rocky outcrops, forests, cultivated land, bare lands, and regions with varying degrees of reforestation, as depicted in Figure 4. This variety in land use contributes to the ecological richness and complexity of the watershed, highlighting the coexistence of natural and anthropogenic elements in the region.

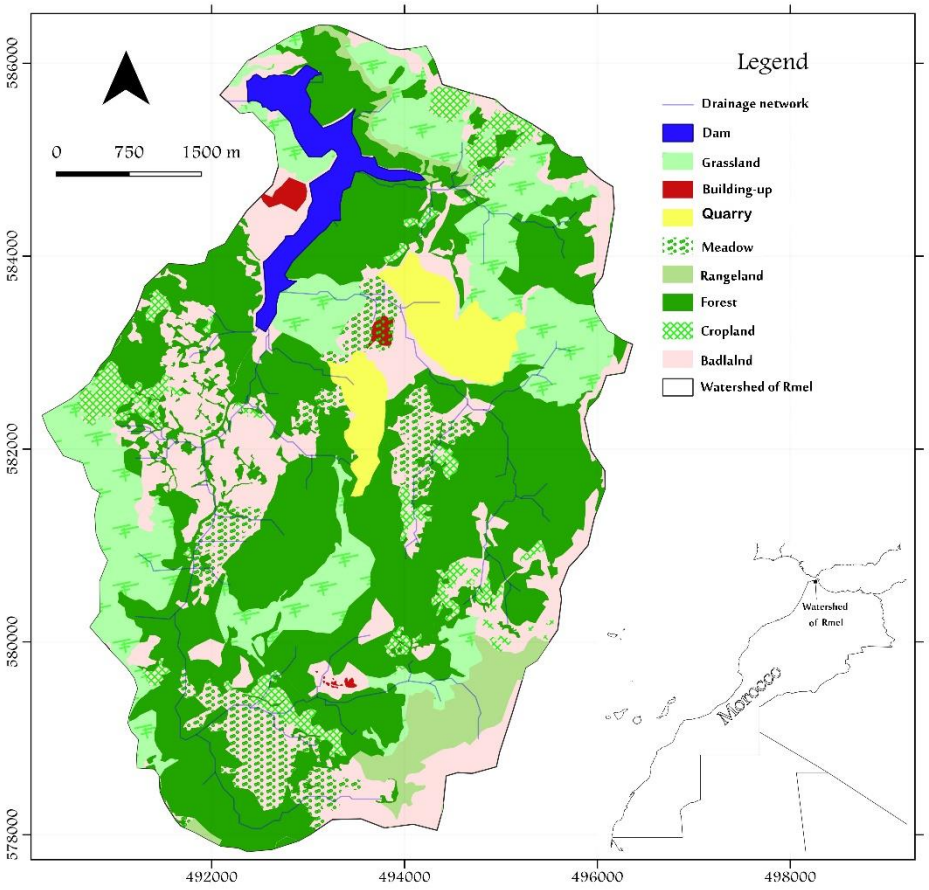

Fig 4: Map of land use in the Rmel basin.

A Digital Terrain Model (DTM) with a spatial resolution of 30m was utilized to augment our understanding of the study area. This DTM facilitated the generation of both a slope map and a flow accumulation map, critical components for the subsequent preparation of the LS factor map in ArcGIS (Rodriguez and Suarez, 2012) (figure 5). The LS factor map, derived from these inputs, serves as a valuable tool in assessing the impact of terrain on soil erosion dynamics, enhancing our capacity to analyse and manage erosion risk within the study region.

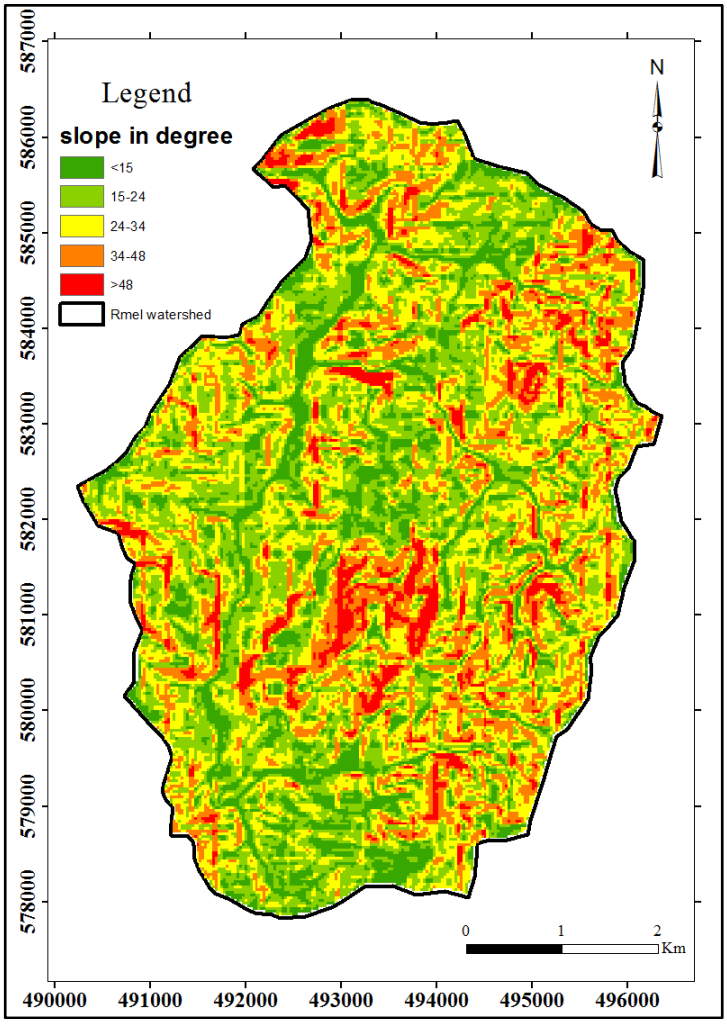

Fig 5. Slope map of the Rmel watershed.

RESULTS AND DISCUSSION

Assessing water erosion factors

The principal objective of this study is to forecast the long-term average annual erosion rate in the Rmel watershed by employing the Revised Universal Soil Loss Equation (RUSLE) model. This predictive model considers various variables, encompassing rainfall patterns, topography, vegetation cover, and agricultural practices.

Rainfall erosivity factor (R)

The kinetic energy of rain plays a substantial role in the removal of solid particles. It is intricately linked to the intensity of the rainfall, influenced by both drop size and velocity (Bartolomé and Teuwen, 2019). The computation of the

climatic aggressivity factor, as proposed by Wischmeier and Smith (1978), relies on the understanding of rain kinetic energy and the average rainfall intensity over a 30-minute duration, expressed by the following formula:

$$\mathbf{R=K*EC*I30} \quad \text{Eq. (2)}$$

where:
R: climatic aggressiveness
K: coefficient depending on the unit of measurement
EC: kinetic energy
I30: average intensity of precipitation over 30 min.

The rainfall erosivity factor is expressed in its of M. mm / ha. h. (Rango and Arnoldus, 1987) devised the most widely utilized formula for estimating the R factor, incorporating monthly and annual rainfall. The formulation is articulated as follows:

$$\mathbf{logR= 1.74* log(Pi^2/P)+1.29} \quad \text{Eq. (3)}$$

where
Pi represents monthly rainfall and P annual rainfall in mm. It is calculated using data from 5 rainfall stations after the results were interpolated over the rest of the basin. The calculation of the erosivity factor R is applied to a series of twelve (12) years of precipitation.

As illustrated in Figure 5, the R-factor values for the Oued Rmel watershed vary between 95.14 and 118.09 M.mm/ha. H (Table 2). The northeastern region exhibits the highest values, whereas the central and southern regions record the lowest values. This spatial pattern indicates increased precipitation aggressiveness from the south to the northeast. This observed gradient is attributed to the altitudinal fluctuations within the watershed, resulting in an elevation-related increment in precipitation levels from the southern to the northeastern regions (Figure 6).

The R-factor values observed in the Oued Rmel watershed ranged from 95.14 to 118.09 M.mm/ha. h, are consistent with findings Ouallali et *al.* (2016) reported for the Oued Arbaa Ayacha watershed in the Western Rif, where values range from 116.633 to 122.615. Comparable patterns are also evident in the Oued Khmis watershed (Western Rif), as reported by Issa *et al.* (2014), with values ranging from 87 to 113. However, the R-factor values in the Oued Rmel watershed surpass those documented in the Oued Leben watershed (central Rif) by Rahhou (1999), where values range from 43 to 87. Dhman *et al.* (1997) identified elevated R-factor values ranging from 215 to 228 in the Telata catchment, and 198.5 to 213 was found in the El Kharoub watershed (Ammari *et al.* 2023).

Table 2: Average annual precipitation (mm) and average R value for 2010-2022.

Station	Average annual precipitation (mm)	R-value
Alian	719.86	112.30
Tanger Med dam	745.69	118.09
Oued Rmel	583.71	96.13
Ksar Essghir	756.78	97.25
El Horra	511.80	95.14

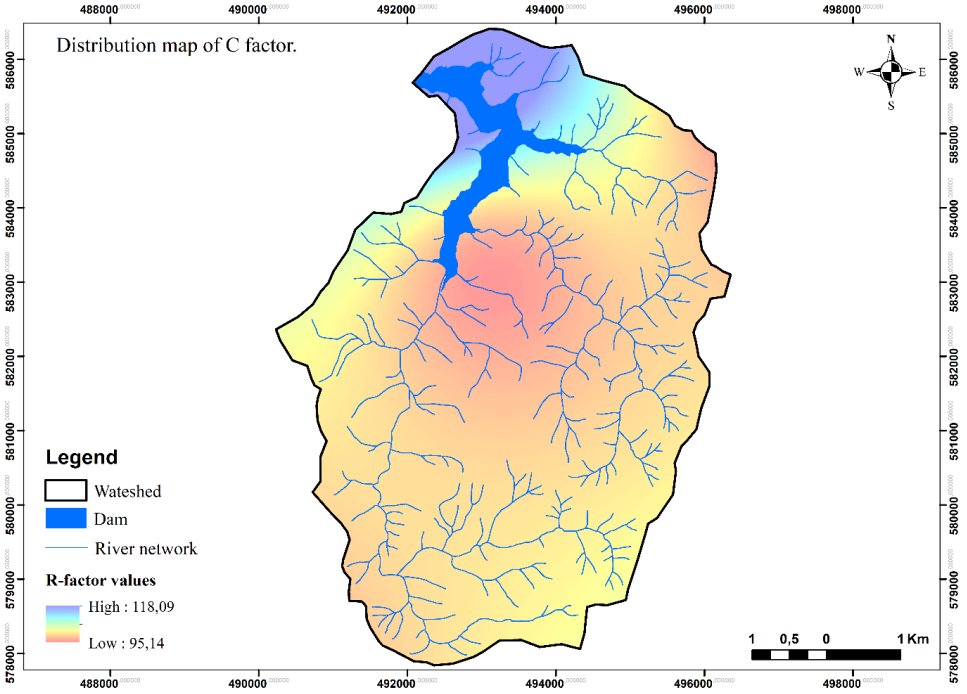

Fig 6: Map of rainfall erosivity factor (R) in the Rmel watershed.

Soil Erodibility Factor (K)

The analysis of pedological properties in the study area facilitated their classification within the Wischmeier and Smith (1978) abacus. This classification was instrumental in estimating the K factor, which is a function of organic matter, structure, texture, and permeability parameters. The K factor holds paramount significance in the Wischmeier and Smith (1978) erosion equation (Eq. 4) as it signifies the degree of soil erodibility, determined through compositional characteristics. The K factor was derived using the following equation (Eq. 4) based on the analysis of soil samples collected within the study area:

$$100K=2.1*M^{1.4}*10^{-4}(12-a)+3.25(b-2)+2.5(c-3) \quad \text{Eq. (4)}$$

with, K: Soil erodibility in ha.H/ha.MJ.mm; M: (% Fine sand +% Silt) *(100-% Clay); a: % organic matter; b: soil structure code (1 to 4): 1: very fine; 2: fine; 3: medium and coarse; 4: very coarse c: permeability code (1 to 6): 1 rapid; 2 medium to rapid; 3 moderate; 4 slow to moderate; 5 slow and 6 very slow.

Determining the K factor in the Oued Rmel watershed involved a comprehensive soil sampling study. This study was conducted within the Rmel watershed, encompassing 16 sites where soil samples were collected at three distinct depths. A meticulous methodology, guided by a geological map, guided the sampling process, resulting in 48 carefully preserved and labeled samples. Subsequently, these samples were analyzed at the INRA Rabat laboratory to ensure precision in assessing the soil parameters essential for calculating the K factor.

In the laboratory, the initial processing of samples involved air-drying, followed by grinding and sieving to obtain particle sizes of 2 mm and 0.2 mm, respectively (Figure 7). Subsequently, these prepared samples underwent a comprehensive series of chemical and physical analyses to ascertain their composition and characteristics. This analytical approach was employed to obtain a thorough understanding of the soil properties necessary to determine the K factor in the Oued Rmel watershed.

Fig 7: Soil sample preparation steps
(1: Air drying, 2: Grinding, 3: 2mm sieving, 4: 0.2mm sieving).

Total carbon and organic matter

The soil samples' organic matter content was assessed using the Walkley and Black (1934) method. This method entails the cold oxidation of the organic carbon fraction using 1N potassium dichromate (K2Cr2O7). An initial sulfuric acid (H2SO4) treatment is conducted to mitigate potential chloride interference that might influence results. Following a 2-hour resting period, the surplus dichromate is titrated using 0.5N Mohr's salt solution (Table 3). The organic matter content (%MO) can then be calculated using the following equation:

$$\mathbf{MO\%=\%C*1.724} \quad \text{Eq. (5)}$$

Table 3: Standards for interpreting organic matter (Walkley and Black, 1934).

Class of MO%	**<1.5**	**1.5-3**	**>3**
Interpretation	Low content	Medium content	High content

Particle size analysis

The physical analysis, known as granulometry, evaluates the sample's size and weight proportions of distinct particle categories (Pye and Blott, 2004). This method classifies soil components based on their diameter, providing valuable insights into the particle distribution within the soil sample (Table 4).

Table 4: Granulometric soil texture scale.

Clays	Fine silts	Coarse silts	Fine sands	Coarse sands	Gravel	Pebbles
< 2µm	2-20µm	20-50µm	50-200µm	200µm-2mm	2-20mm	>20mm

Particle size analysis followed the O.R.S.T.O.M (Office of Scientific and Technical Research Outre-Mer, 1937) standard method. This protocol is a well-established procedure designed to ascertain the particle size distribution within a given sample, providing a standardized and reliable approach for characterizing the soil's granulometric composition.

The determined K factor values for the Rmel watershed vary from 0.088t.ha.h/ha.MJ.mm for the most resistant soils to 0.65 t.ha.h/ha.MJ.mm for the most erodible soils. The resulting map illustrates that the soils exhibiting the highest susceptibility to water erosion (K > 0.36 t.ha.MJ.mm/ha) predominantly belong to the class of Vertisols (Table 5).

Vertisols are fertile clay soils known for their high water retention capacity, and they form a distinct band in the central region, roughly oriented from northeast to southwest (Figure 8).

Table 5: Results of the particle size analysis of the samples and value of the K factor

X	Y	%OM(a)	Texture			Texture	K value
			% Sand	% Silt	% Clay		
-5.44618	35,86744	4.3	21.9	34.1	44.0	Clayey	0.17
-5.48867	35,84242	0.1	14.6	40.0	45.4	Clayey	0.25
-5.4896	35,8463	3.4	11.9	52.3	35.8	Clay silt	0.28
-5.48581	35,84874	5.0	18.2	35.6	46.1	Clayey	0.14
-5.48333	35,85681	2.7	8.1	42.9	49.1	Clay sand	0.16
-5.48179	35,86209	3.2	64.5	20.7	14.8	Silt sand	0.62
-5,46294	35,86211	0.6	19.6	34.9	45.6	Clay sand	0.23
-5.46856	35,85608	3.7	21.6	34.6	43.8	Clayey	0.19
-5.47238	35,85372	0.2	27.9	47.0	25.1	Silt	0.58
-5.46551	35,84751	2.0	24.4	56.0	19.6	Silt	0.60
-5,47196	35,84555	0.4	18.1	44.8	37.1	Clay silt	0.35
-5.48735	35,83083	4.1	12.4	47.1	40.5	Clay silt	0.21
-5.47319	35,81139	5.3	9.9	36.0	54.1	Clayey	0.088
-5.47435	35,82016	0.5	54.3	24.4	21.3	Sand	0.65
-5.48655	35,82375	4.9	25.4	30.9	43.7	Clayey	0.16
-5.45976	35,86665	3.5	21.2	35.3	43.5	Clayey	0.19

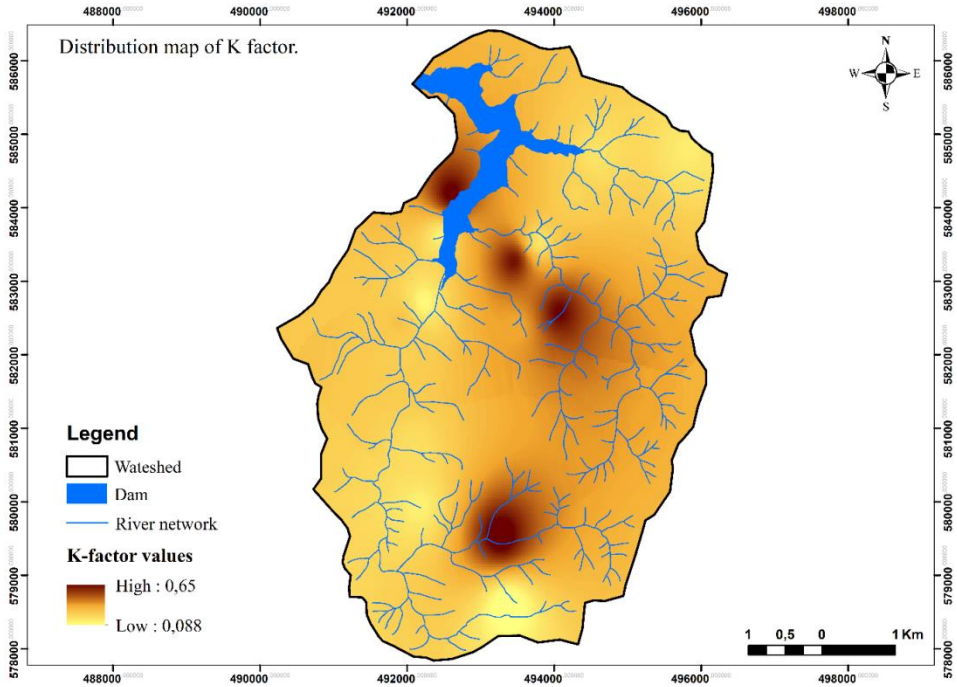

Fig 8: Map of Soil erodibility factor (K) in the Rmel watershed.

Topographic Factor (LS)

The LS factor, commonly known as the "topographic factor," serves as a measure of how the erosion process is influenced by the length of the slope (L) and the steepness of the slope (S) (Anjitha *et al.* 2019). As expressed by the LS factor, these slope-related variables play a pivotal role in shaping the generation and movement of sediment on slopes (Roose 1994). Notably, there is a concurrent increase in soil erosion when development occurs along a slope. The slope's steepness further intensifies this escalation. Moreover, the quantity of vegetation and the size of soil particles influence the dynamics of this soil erosion relationship. The LS factor is mathematically expressed by the following equation (Wischmeier and Smith, 1978):

$$LS = L \div 22.13^{m} \times (0.065 + 0.045S + 0.0065S^{2}) \quad \text{Eq. (6)}$$

where L: slope length, S: slope (%), m: constant dep. on slope value (Tab. 6).

Table 6: The relationship between the parameter m and slope.

Slope (%)	S ≤1	1<S ≤3	3<S ≤5	S>5
m	0.2	0.3	0.4	0.5

The multiplication of flow accumulation and resolution, derived from a digital terrain model, yields slope length (Bircher *et al.* 2019). The ArcGIS Spatial Analyst tool performed slope and flow accumulation computations on the ASTER digital model.

The LS factor calculation reveals a range from 0 to 609.9 (Figure 9) across altitudes spanning 12m to 408m and slopes from 15% to 48%. Elevated LS values predominantly correspond to specific river segments and high-altitude regions characterized by steep slopes. These regions are primarily situated in the central and peripheral zones of the watershed.

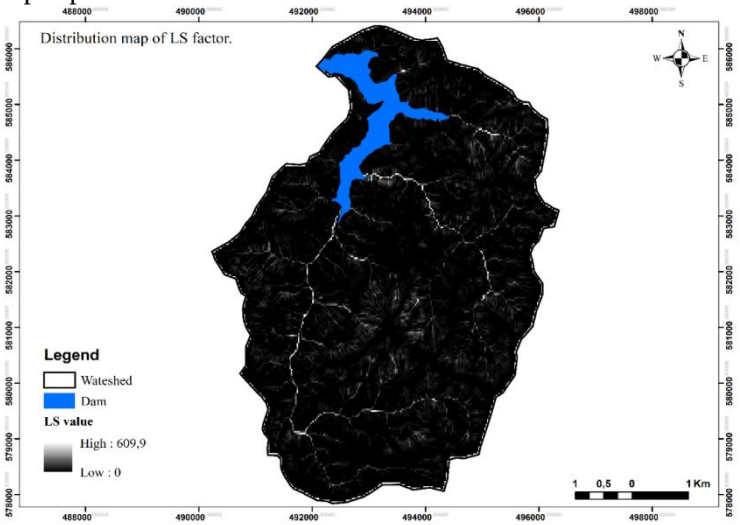

Fig 9. Map of Topographic Factor (LS).

Vegetation cover factor (C)

The influence of vegetation cover is quantified through a dimensionless factor obtained from the normalized vegetation index (NDVI) derived from satellite imagery. This index translates vegetation reflectance into a percentage of vegetation cover (Khunrattanasiri, 2023). However, in response to seasonal canopy variations, our study employs an alternative method, replacing the traditional C-factor with the NDVI vegetation index (Macedo *et al.* 2021).

For our investigation, NDVI is computed from Landsat 8 OLI images at a spatial resolution of 30m. It is utilized to assess the spectral signature, encompassing the near-infrared portion of the electromagnetic spectrum and the red reflection in the upper visible spectrum. The relationship between NDVI and C is expressed by the following equation (Prasannakumar *et al.* 2012):

$$\mathbf{C = exp(-a\ NDVI/(\beta\text{-}NDVI))} \quad \text{Eq. (7)}$$

The C factor spans from 0.1 to 1 (Figure 10). The spatial distribution of these values reveals that 43% of the catchment area exhibits a vegetation cover ranging from low to moderate, with a C factor greater than 0.2. In contrast, 57% of the area seems adequately protected, featuring C values below 0.2, indicating a high level of preservation. These areas encompass virtually the entire basin.

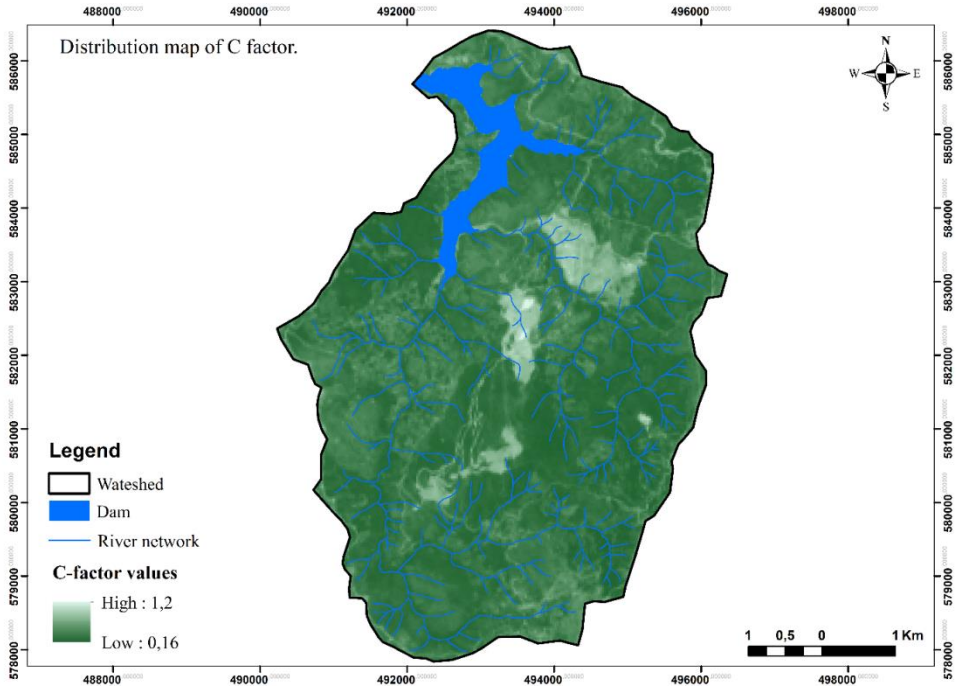

Fig 10. Distribution map of C factor in the watershed

Pratique de gestion des terres factor (P)

The soil conservation practice factor, also called the support practice, indicates the proportion of soil loss assigned to each cultivation method based on its ability to conserve soil from erosion (Panagos *et al.* 2015). This includes contour plowing, ridging, slope terracing, and alternating strip crops. The P factor evaluates the impact of conservation tillage on reducing soil loss (Araya *et al.* 2011). If adequately maintained, erosion control measures influence water flow and land topography, reducing soil loss. The P factor is assigned a value between 0 and 1, where 1 signifies the absence of conservation features.

This metric facilitates the assessment of soil losses in watersheds by considering the effectiveness of existing erosion control techniques. Each measure has a protective degree, with its coefficient determined by how well it minimizes runoff and mitigates erosion causes (Benzougagh *et al.* 2020). Cultivation practices such as contour farming, alternating strips or terraces, reforestation on terraces, and ridging are identified as highly effective soil conservation strategies (Zettam *et al.* 2022). These strategies are evaluated based on the soil loss ratio with specific support on agricultural land compared to the corresponding loss with parallel slope plowing (Zouagui *et al.* 2018).

It is essential to highlight that in our study, areas with low to moderate slopes exhibit the lowest and average P-factor values. Specifically, the P factor ranges between 0.2 and 0.5 for areas with low slopes, while it varies between 0.6 and 0.9 for areas with steep slopes (Figure 11).

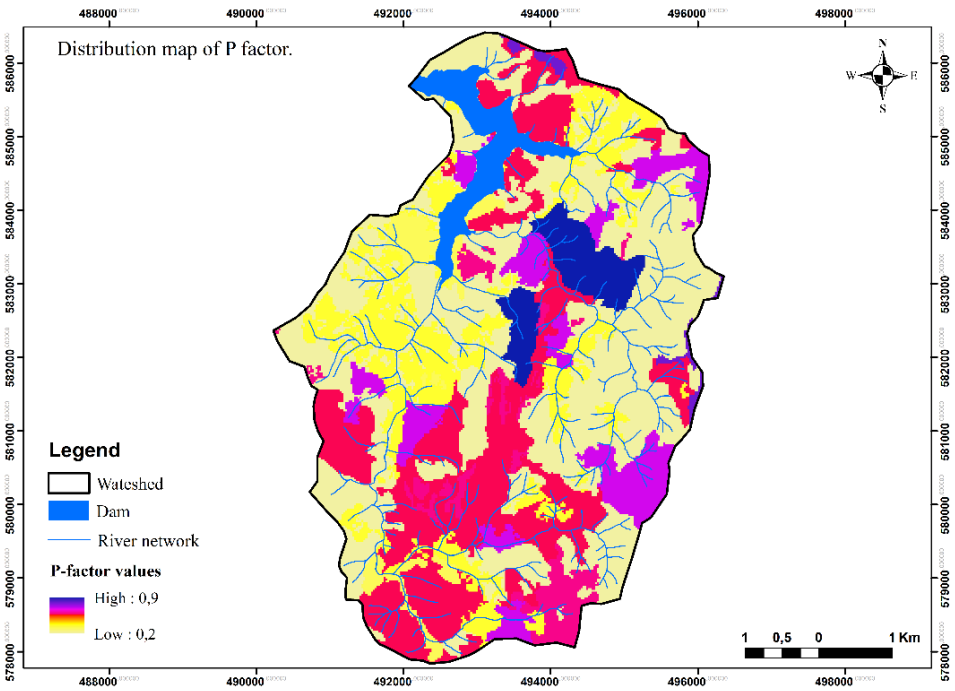

Fig 11: Map of the anti-erosion factor (P) in the watershed Rmel

Erosion rate estimation

The erosion rate, as determined by the RUSLE model, results from the interplay of various factors, with climatic aggressiveness (R), soil erodibility (K), and the combined impact of slope degree and slope length (LS), vegetation cover (C), and erosion control practices (P) being the most influential. Calculating the erosion rate provides insights into the distribution of erosion risk attributable solely to natural factors.

The results indicate a range of soil losses in the region, spanning from less than 7 to over 45 t/ha/year, with an average of approximately 16 t/ha/year. Approximately 60% of the basin area falls within the loss class below 7 t/ha/year, signifying relatively low losses. About 30% of the area is categorized as having moderate losses, falling between 7 and 20 t/ha/year. Areas experiencing high water erosion, exceeding 20 t/ha/year, constitute only 10% of the total Rmel watershed area. These vulnerable zones to water erosion are predominantly situated in the central and north-eastern portions of the watershed (Figure 12).

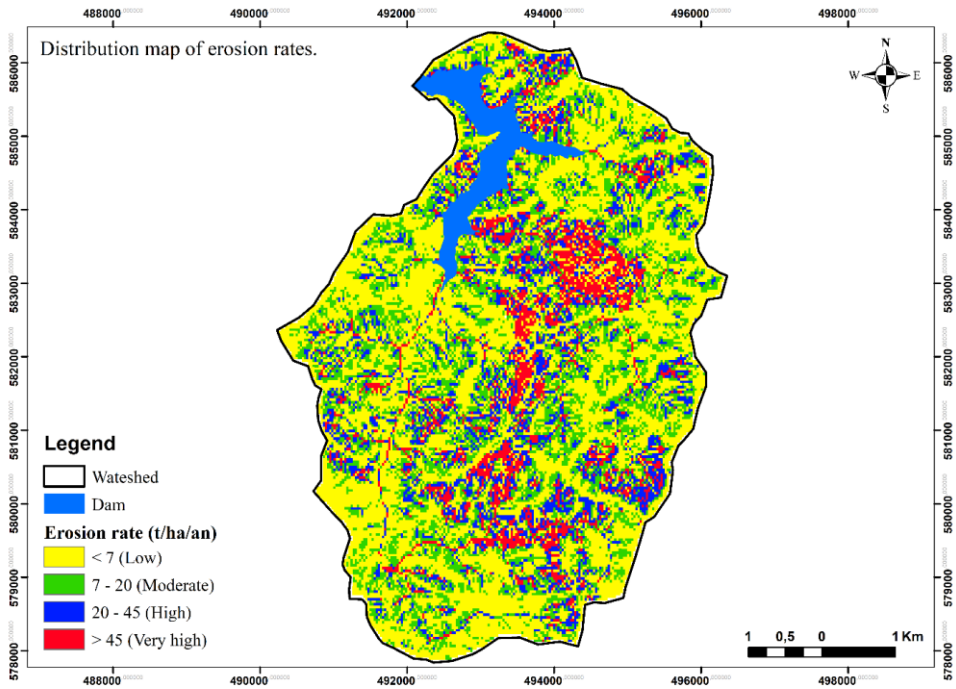

Fig 12: Resulting map of soil losses in t/ha/yr

The areas with a high potential for erosion are typically associated with soils in the central basin regions characterized by steep slopes and intense human activity, particularly quarrying. In the northeastern part, precipitation (climatic aggressiveness) emerges as the primary factor driving water erosion despite relatively abundant vegetation.

On the Rif scale, the Rmel watershed stands out for having the best protection against water erosion. Specifically, the Sania and Arbaa Ayacha watersheds in the western Rif exhibit an average annual loss of approximately 47.18 t/ha (Tahiri *et al.* 2015) and 25.8 t/ha (Ouallali *et al.* 2016), respectively. Comparable values were observed in the eastern Rif, with the Oued Sahla basin recording 22 t/ha/yr and the Oued Boussouabl basin registering 55 t/ha/yr (Sadiki *et al.* 2009).

CONCLUSION

The RUSLE approach for assessing soil water erosion indicates that the Rmel watershed faces a relatively low erosion risk compared to other regions in the Rif. Areas with susceptible soils encompass only 9% of the basin area, exhibiting an average annual erosion rate exceeding 15 t/ha. These vulnerable zones, predominantly situated in the central and downstream parts of the basin, show that human activities and climatic aggressiveness are the primary contributors to soil erosion. On the other hand, areas with low erosion potential, as inferred from land loss estimates, are mainly characterized by cultivated land featuring a topography dominated by low slope classes and experiencing low rainfall erosivity.

The optimized RUSLE equation developed in this analysis could be a valuable resource for future regional land-use planning and management activities; however, caution is advised in its application. Furthermore, it provides a framework for potential soil erosion studies in the study area and other similarly conditioned regions. To calculate the rate of soil loss in the watershed, alternative techniques such as radioactive markers like Caesium 137 (137Cs), PAP/CAR, the SWAT model (Soils Water Assessment Tools), the IntErO model (Spalevic, 2011), River Basins model (Spalevic, 1999) and the SAM model (Spectral Angel Mapper) could also be considered.

REFERENCES

Ammari, Z., El Mostafa Mili, A. E., El Hafyani, M., Essahlaoui, N., Boufala, M. H., Ouallali, A., Berrad, F., & Aassoumi, H. (2023). Mapping and predicting of water erosion using RUSLE in the mediterranean context: case of El Kharroub watershed (western rif, northern morocco). ARPN Journal of Engineering and Applied Sciences, 18,6.

Anjitha Krishna, P. R., Lalitha, R., Shanmugasundaram, K., & Nagarajan, M. (2019). Assessment of topographical factor (LS-factor) estimation procedures in a gently sloping terrain. Journal of the Indian Society of Remote Sensing, 47, 1031-1039.

Araya, T., Cornelis, W. M., Nyssen, J., Govaerts, B., Bauer, H., Gebreegziabher, T., & Deckers, J. (2011). Effects of conservation agriculture on runoff, soil loss and crop yield under rainfed conditions in Tigray, Northern Ethiopia. Soil Use and Management, 27(3), 404-414.

Bartolomé, L., & Teuwen, J. (2019). Prospective challenges in the experimentation of the rain erosion on the leading edge of wind turbine blades. Wind Energy, 22(1), 140-151.

Benzougagh, B., Meshram, S. G., Baamar, B., Dridri, A., Boudad, L., Sadkaoui, D., & Mimich, K. (2020). Relationship between landslide and morpho-structural analysis: a case study in Northeast of Morocco. Applied Water Science, 10(7), 1-10.

Bezak, N,; Mikoš, M.; Borrelli, P.; Alewell, C.; Alvarez, P.; Alexandre Ayach Anache, J.; Baartman, J.; Ballabio, C.; Biddoccu, M.; Cerdà, A.; Chalise, D.; Chen, S.; Chen, W.; De Girolamo, A.; Desta Gessesse, G.; Deumlich, D.; Diodato, N.; Efthimiou, N.; Erpul, G.; Fiener, P.; Freppaz, M.; Gentile, F.; Gericke, A.; Haregeweyn, N.; Hu, B.; Jeanneau, A.; Kaffas, K.; Kiani-Harchegani, M.; Lizaga Villuendas, I.; Li, C.; Lombardo, L.; López-Vicente, M.; Esteban Lucas-Borja, M.; Maerker, M.; Miao, C.; Modugno, S.; Möller, M.; Naipal, V.; Nearing, N.; Owusu, S.; Panday, D.; Patault, E.; Valeriu Patriche, C.; Poggio, L.; Portes, R.; Quijano, L.; Reza Rahdari, M.; Renima, M.; Francesco Ricci, G.; Rodrigo-Comino, J.; Saia, S.; Nazari Samani, A.; Schillaci, C.; Syrris, V.; Soo Kim, H.; Noses Spinola, D.; Tarso Oliveira, P.; Teng, H.; Thapa, R.; Vantas, K.; Vieira, D.; Yang, J.; Yin, S.; Antonio Zema, D.; Zhao, G. & Panagos, P. (2021). Soil erosion modelling: A bibliometric analysis. Environmental Research, 197, 111087

Bhat, S. A., Dar, M. U. D., & Meena, R. S. (2019). Soil erosion and management strategies. Sustainable management of soil and environment, 73-122.

Bircher, P., Liniger, H. P., & Prasuhn, V. (2019). Comparing different multiple flow algorithms to calculate RUSLE factors of slope length (L) and slope steepness (S) in Switzerland. Geomorphology, 346, 106850.

Briak, H., Moussadek, R., Aboumaria, K., & Mrabet, R. (2016). Assessing sediment yield in Kalaya gauged watershed (Northern Morocco) using GIS and SWAT model. International Soil and Water Conservation Research, 4(3), 177-185.

Djoukbala, O., Hasbaia, M., Benselama, O., & Mazour, M. (2019). Comparison of the erosion prediction models from USLE, MUSLE and RUSLE in a Mediterranean watershed, case of Wadi Gazouana (NW of Algeria). Modeling Earth Systems and Environment, 5(2), 725-743.

Ed-daoudy, L., Lahmam, N., Benmansour, M., Afilal, H., & Damnati, B. (2023). Hydric erosion rates in Raouz watershed, Morocco: RUSLE, GIS, and remote sensing. Remote Sensing Applications: Society and Environment, 32, 101056.

El Jazouli, A., Barakat, A., Khellouk, R., Rais, J., & El Baghdadi, M. (2019). Remote sensing and GIS techniques for prediction of land use land cover change effects on soil erosion in the high basin of the Oum Er Rbia River (Morocco). Remote Sensing Applications: Society and Environment, 13, 361-374.

Fartas, N., El Fellah, B., Mastere, M., Benzougagh, B., & El Brahimi, M. (2022). Potential Soil Erosion Modeled with RUSLE Approach and Geospatial Techniques (GIS Tools and Remote Sensing) in Oued Joumouaa Watershed (Western Prerif-Morocco). The Iraqi Geological Journal, 47-61.

García-Ruiz, J. M., Nadal-Romero, E., Lana-Renault, N., & Beguería, S. (2013). Erosion in Mediterranean landscapes: changes and future challenges. Geomorphology, 198, 20-36.

Guzmán, G., Quinton, J. N., Nearing, M. A., Mabit, L., & Gómez, J. A. (2013). Sediment tracers in water erosion studies: current approaches and challenges. Journal of Soils and Sediments, 13, 816-833.

Gwapedza, D., Hughes, D. A., & Slaughter, A. R. (2018). Spatial scale dependency issues in the application of the Modified Universal Soil Loss Equation (MUSLE). Hydrological Sciences Journal, 63(13-14), 1890-1900.

Ibrahim, D., Ahmed, B., Habiba, A., Abdessalam, O., & Youssef, A. B. (2020). Contribution of geophysics to the study of Barite mineralization in the Paleozoic formations of Asdaf Tinejdad (Eastern Anti Atlas Morocco). Economic and Environmental Geology, 53(3), 259-269.

Issa, L. K., Raissouni, A., Moussadek, R., El ArrimIssa, A., Khali, L., Raissouni, A., ... & El Arrim, A. (2014). Mapping and assessment of water erosion in the Khmiss Watershed (North Western Rif, Morocco). Current Advances in Environmental Science, 2(4), 119-130.

Karydas, C. G., Panagos, P., & Gitas, I. Z. (2014). A classification of water erosion models according to their geospatial characteristics. International Journal of Digital Earth, 7(3), 229-250.

Kavian, A.; Gholami, L.; Mohammadi, M.; Spalevic, V.; & Falah Soraki, M. (2018). Impact of Wheat Residue on Soil Erosion Processes. Notulae Botanicae Horti Agrobotanici Cluj-Napoca, 46(2), 553-562.

Khunrattanasiri, W. (2023). Application of Remote Sensing Vegetation Indices for Forest Cover Assessments. In Concepts and Applications of Remote Sensing in Forestry (pp. 153-166). Singapore: Springer Nature Singapore.

Macedo, P. M. S., Oliveira, P. T. S., Antunes, M. A. H., Durigon, V. L., Fidalgo, E. C. C., & de Carvalho, D. F. (2021). New approach for obtaining the C-factor of RUSLE considering the seasonal effect of rainfalls on vegetation cover. International soil and water conservation research, 9(2), 207-216.

Millward, A. A., & Mersey, J. E. (1999). Adapting the RUSLE to model soil erosion potential in a mountainous tropical watershed. Catena, 38(2), 109-129.

Moukhchane, M., Bouhiassa, S., & Chalouan, A. (1998). Approche cartographique et magnétique pour l'identification des sources de sédiments: cas du bassin versant Nakhla (Rif, Maroc). Science et changements planétaires/Sécheresse, 9(3), 227-232.

Mukanov, Y., Chen, Y., Baisholanov, S., Amanambu, A. C., Issanova, G., Abenova, A., ... & Abayev, N. (2019). Estimation of annual average soil loss using the Revised Universal Soil Loss Equation (RUSLE) integrated in a Geographical Information System (GIS) of the Esil River basin (ERB), Kazakhstan. Acta Geophysica, 67, 921-938.

Ouallali, A., Aassoumi, H., Moukhchane, M., Moumou, A., Houssni, M., Spalevic, V., & Keesstra, S. (2020). Sediment mobilization study on Cretaceous, Tertiary and Quaternary lithological formations of an external Rif catchment, Morocco. Hydrological Sciences Journal, 65(9), 1568-1582.

Ouallali, A., Briak, H., Aassoumi, H., Beroho, M., Bouhsane, N., & Moukhchane, M. (2020). Hydrological foretelling uncertainty evaluation of water balance components and sediments yield using a multi-variable optimization approach in an external Rif's catchment. Morocco. Alexandria Engineering Journal, 59(2), 775-789.

Ouallali, A., Moukhchane, M., Aassoumi, H., Berrad, F., Ibrahim, D., (2016). Evaluation and mapping of water erosion rates in the watershed of the Arbaa Ayacha river (western Rif, northern Morocco). Bull. Inst. Sci. Sect. Sci. Terre 38, 65–79.

Ouallali, A.; Bouhsane, N.; Bouhlassa, S.; Moukhchane, M.; Ayoubi, S.; Aassoumi, H. Rapid magnetic susceptibility measurement as a tracer to assess the erosion-deposition process using tillage homogenization and simple proportional models: A case study in northern of Morocco. International Journal of Sediment Research. (2023), 38, 739–753.

Panagos, P., Borrelli, P., Meusburger, K., Van Der Zanden, E. H., Poesen, J., & Alewell, C. (2015). Modelling the effect of support practices (P-factor) on the reduction of soil erosion by water at European scale. Environmental science & policy, 51, 23-34.

Prasannakumar, V., Vijith, H., Abinod, S., & Geetha, N. J. G. F. (2012). Estimation of soil erosion risk within a small mountainous sub-watershed in Kerala, India, using Revised Universal Soil Loss Equation (RUSLE) and geo-information technology. Geoscience frontiers, 3(2), 209-215.

Pye, K., & Blott, S. J. (2004). Particle size analysis of sediments, soils and related particulate materials for forensic purposes using laser granulometry. Forensic Science International, 144(1), 19-27.

Rahhou, M. (1999). L'érosion dans le Prérif central, zone interfluviale Leben-Sebou-Ouergha, un prolongement de l'évolution naturel, une production sociale. State thesis, Mohammed V University of Rabat, Morocco.

Rango, A., & Arnoldus, H. M. J. (1987). Watershed management. Food and Agriculture Organization Technical Papers. Rome. FAO, 36.

Rodrigues Neto, M.R.; Musselli, D.G.; Lense, G.H.E.; Servidoni, L.E.; Stefanidis, S.; Spalevic, V.; Mincato, R.L. (2022). Soil loss modelling by the IntErO model - Erosion Potential Method in the Machado River Watershed, Minas Gerais, Brazil. Agriculture and Forestry, 68 (2): 7-21.

Rodriguez, J. L. G., & Suarez, M. C. G. (2012). Methodology for estimating the topographic factor LS of RUSLE3D and USPED using GIS. Geomorphology, 175, 98-106.

Römkens, M. J., Wells, R. R., Wang, B., Zheng, F., & Hickey, C. J. (2015). Soil Erosion on Upland Areas by Rainfall and Overland Flow. Advances in Water Resources Engineering, 361-405.

Roose, E. (1994). Introduction à la gestion conservatoire de l'eau, de la biomasse et de la fertilité des sols (GCES) (Vol. 70). Organisation des Nations Unies pour l'alimentation et l'agriculture.

Roose, E. (2002). Traditional strategies for soil and water conservation in Mediterranean areas. Rubio, Josè Luis.

Sabri, E., Spalevic, V., Boukdir, A., Karaoui, I., Ouallali, A., Mincato, R. L., & Sestras, P. (2022). Estimation of soil losses and reservoir sedimentation: a case study in Tillouguite sub-basin (high Atlas-Morocco). Agriculture & Forestry/Poljoprivreda i Sumarstvo, 68(2).

Sadiki, A., Faleh, A., Zêzere, J. L., & Mastass, H. (2009). Quantification de l'Erosion en Nappes dans le Bassin Versant de l'Oued Sahla-Rif Central Maroc. Cahiers géographiques, 6, 59-70.

Saikumar, G., Pandey, M., & Dikshit, P. K. S. (2022). Natural River Hazards: Their Impacts and Mitigation Techniques. In River Dynamics and Flood Hazards: Studies on Risk and Mitigation (pp. 3-16). Singapore: Springer Nature Singapore.

Sakuno, N. R. R., Guiçardi, A. C. F., Spalevic, V., Avanzi, J. C., Silva, M. L. N., & Mincato, R. L. (2020). Adaptation and application of the erosion potential method for tropical soils. Revista Ciência Agronômica, 51.

Salhi, A., Benabdelouahab, T., Hasnaoui, Y. E., El Moussaoui, M., El Morabit, A., Himi, M., ... & Martin-Vide, J. (2021). Soil erosion assessment and farmers' perception in south Mediterranean basins: a Moroccan case study. In Recent Advances in Environmental Science from the Euro-Mediterranean and Surrounding Regions (2nd Edition) Proceedings of 2nd Euro-Mediterranean Conference for Environmental Integration (EMCEI-2), Tunisia 2019 (pp. 2019-2024). Springer International Publishing.

Salhi, A., El Hasnaoui, Y., Pérez Cutillas, P., & Heggy, E. (2023). Soil erosion and hydroclimatic hazards in major African port cities: the case study of Tangier. Scientific Reports, 13(1), 13158.

Spalevic, V. (1999). Application of computer-graphic methods in the studies of draining out and intensities of ground erosion in the Berane valley. Master thesis, Faculty of Agriculture of the University of Belgrade, Serbia, 1999: 135p.

Spalevic, V. (2011). Impact of land use on runoff and soil erosion in Polimlje. Doctoralthesis, University of Belgrade, Faculty of Agriculture, Serbia, p 1-260.

Spalevic, V., Djurovic, N., Mijovic, S., Vukelic-Sutoska, M., & Curovic, M. (2013). Soil erosion intensity and runoff on the Djuricka River Basin (North of Montenegro). Malaysian Journal of Soil Science, 17(1), 49-68.

Stefanidis, S., Alexandridis, V., Spalevic, V., Mincato, R.L. (2022). Wildfire Effects on Soil Erosion Dynamics: The Case of 2021 Megafires in Greece. Agriculture and Forestry, 68 (2): 49-63. doi:10.17707/AgricultForest.68.2.04

Tahiri, M., Tabyaoui, H., Tahiri, A., El Hadi, H., El Hammichi, F., & Achab, M. (2015). Modelling soil erosion and sedimentation in the Oued Haricha sub-basin (Tahaddart watershed, Western Rif, Morocco): risk assessment. Journal of Geoscience and Environment Protection, 4(1), 107-119.

Walkley, A., & Black, I. A. (1934). An examination of the Degtjareff method for determining soil organic matter, and a proposed modification of the chromic acid titration method. Soil science, 37(1), 29-38.

Wischmeier, W. H., & Smith, D. D. (1978). Predicting rainfall erosion losses: a guide to conservation planning (No. 537). Department of Agriculture, Science and Education Administration.

Zettam, A., Briak, H., Kebede, F., Ouallali, A., Hallouz, F., & Taleb, A. (2022). Efficiencies of best management practices in reducing nitrate pollution of the Sebdou River, a semi-arid Mediterranean agricultural catchment (North Africa). River Research and Applications, 38(3), 613-624.

Zhang, Y., Degroote, J., Wolter, C., & Sugumaran, R. (2009). Integration of modified universal soil loss equation (MUSLE) into a GIS framework to assess soil erosion risk. Land Degradation & Development, 20(1), 84-91.

Zouagui, A., Sabir, M., Naimi, M., Chikhaoui, M., & Benmansour, M. (2018). Modélisation du risque d'érosion hydrique par l'équation universelle des pertes en terre dans le Rif Occidental: Cas du bassin versant de Moulay Bouchta (Maroc). European Scientific Journal, 14(3), 1857-788.